Energy Transfer Dynamics in Light-Harvesting Assemblies Templated by the Tobacco Mosaic Virus Coat Protein

Ying-Zhong Ma,[†] Rebekah A. Miller,[‡] Graham R. Fleming,[†] and Matthew B. Francis*[,‡]

Department of Chemistry, University of California, Berkeley, and Physical Biosciences Division, Lawrence Berkeley National Laboratory, Berkeley, California 94720-1460, and Department of Chemistry, University of California, Berkeley, California 94720-1460, and Materials Sciences Division, Lawrence Berkeley National Laboratory, Berkeley, California 94720-1460

Received: January 22, 2008; Revised Manuscript Received: March 7, 2008; In Final Form: March 19, 2008

Picosecond time-resolved fluorescence spectroscopy was used to characterize energy transfer between chromophores displayed on a rod assembly of tobacco mosaic virus coat protein. The incorporation of donor chromophores with broad and overlapping absorption and emission spectra creates an "antenna" with a large absorption cross section, which can convey excitation energy over large distances before transfer to an acceptor chromophore. The possibility for both donor-to-donor and donor-to-acceptor transfer results in complex kinetic behavior at any single wavelength. Thus, to describe the various pathways of energy transfer within this system accurately, a global lifetime analysis was performed to obtain decay associated spectra. We found the energy transfer from donor to acceptor chromophores occurs in 187 ps with an efficiency of 36%. A faster decay component of 70 ps was also observed from global lifetime analysis and is attributed to donor-to-donor transfer. Although more efficient three-chromophore systems have been demonstrated, a two-chromophore system was studied here to facilitate analysis.

Introduction

The mechanisms by which photosynthetic organisms use sunlight to create membrane potential and form chemical bonds provide inspiration for the development of solar energy devices. The first step of the photosynthetic process is the absorption of light by an ordered array of carotenoid and (bacterio-)chlorophyll (BChl) molecules organized in light harvesting (LH) antenna complexes.[1] The resulting electronic excitation energy transfers rapidly to the reaction center (RC), where charge separation occurs.[2,3] Extensive studies employing ultrafast optical spectroscopies have revealed the pathways and time scales of excitation energy transfer within and among the various photosynthetic complexes.[3–5] In purple bacteria, for example, BChls are organized into ring structures with distinct interpigment spacing and molecular orientation.[6–9] These structural variations give rise to remarkably different time scales of energy transfer, ranging from 100 fs for the ring composed of strongly interacting BChls to 1.5 ps for the inter-ring processes.[10–12]

Synthetic mimics of this LH antenna architecture have great potential for incorporation in devices, such as solar and fuel cells. To maximize efficiency, the design of these artificial systems should incorporate those parameters found to be essential in the natural photosynthetic apparatus.[13–19] For example, chromophores should have a sufficiently large absorption cross section for efficient photon capture, and they should be positioned such that their orientation and spacing maximizes energy transfer. Additionally, due to their synthetic origin, these systems can offer important advantages over the direct use of biological components, such as improved stability and durability.

It was recently demonstrated that self-assembling proteins, such as the tobacco mosaic virus coat protein (TMVP),[20] can serve as scaffolds for the construction of highly efficient light-harvesting arrays.[21,22] In one study,[21] steady-state spectroscopic experiments were used to evaluate chromophore compositions and donor-to-acceptor ratios. It was found that excitation energy from multiple donor chromophores could be transferred to a single acceptor chromophore. A particularly attractive feature of this system is its ability to use donor chromophores with overlapping excitation and emission spectra, thus allowing donor-to-donor transfer events to convey absorbed energy over long distances.

Because self-assembling proteins represent a new synthetic approach to the construction of artificial LH systems, understanding the energy transfer dynamics is important for further optimization. In a different study by Endo et al.,[22] time-resolved spectroscopy was employed to probe a similar TMV-based system in which the donor chromophore was a Zn-coordinated porphyrin (ZnP) and the acceptor chromophore was a free-base porphyrin.[21] This system represents an important step forward, as porphyrins are more reminiscent of biological chromophores. In this system, lack of appreciable overlap between the ZnP excitation and emission bands minimizes the possibility for donor-to-donor transfer. Thus, time-resolved studies of transfer dynamics were limited to donor-to-acceptor pathways. Even in this more simplified case, the most efficient rod systems proved challenging to fit using the analysis presented, which the authors attributed to processes such as layer-by-layer or stepwise energy transfer.

In the interest of obtaining a more comprehensive understanding of energy transfer in systems with both donor-to-donor and donor-to-acceptor pathways, we used picosecond time-resolved fluorescence spectroscopy to characterize a TMV-based light harvesting system in which the donor was Oregon Green 488 (OG) and the acceptor was Alexa Fluor 594 (AF). The use

* Corresponding author. E-mail: francis@cchem.berkeley.edu.
[†] University of California, Berkeley, and Physical Biosciences Division, Lawrence Berkeley National Laboratory.
[‡] University of California, Berkeley, and Materials Sciences Division, Lawrence Berkeley National Laboratory.

10.1021/jp8006393 CCC: $40.75
Published on Web 05/10/2008

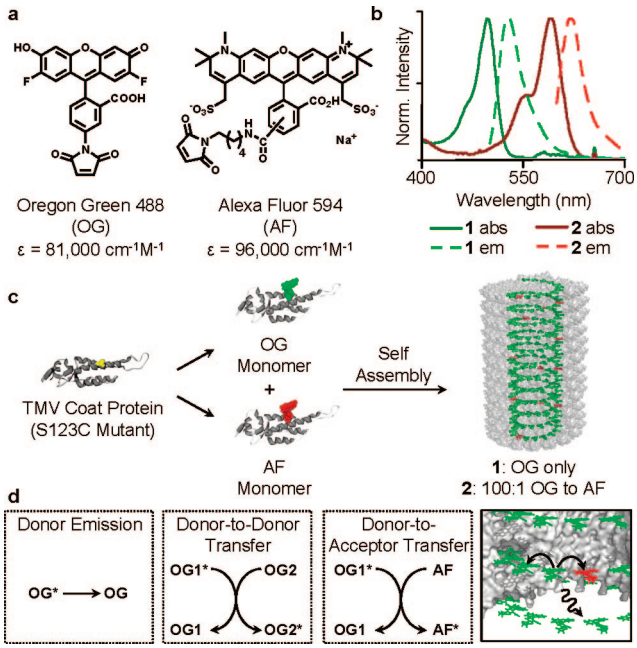

Figure 1. The construction of light harvesting structures containing a 100:1 ratio of donor and acceptor. (a) Chemical structures of the donor chromophore (OG) and the acceptor chromophore (AF). (b) Normalized absorption and emission spectra for OG and AF. (c) C123 TMVP monomers labeled with either OG or AF were combined in a 100:1 ratio before equilibration under rod-forming conditions. Rods containing only OG were also prepared. (d) The three pathways for the dissipation of electronic energy from the donor chromophore excited state include donor emission, donor-to-donor transfer, and donor-to-acceptor transfer.

of chromophores with overlapping emission bands results in complex kinetic behavior at any single wavelength, complicating the analysis significantly.[23,24] Thus, to describe the various pathways of energy transfer within this system accurately (Figure 1d), a global lifetime analysis[25] was undertaken to obtain decay-associated spectra,[26] allowing for characterization of both donor-to-donor and donor-to-acceptor energy transfer events in terms of rate and efficiency.

Results and Discussion

Rod assemblies of TMVP labeled with donor only (**1**) or a 100:1 ratio of donor to acceptor (**2**) were constructed as described previously (Figure 1).[20] The 100:1 ratio was selected to maximize the number of acceptor dyes that were completely surrounded by donors. Briefly, monomeric S123C TMVP was singly modified with either OG or AF using cystine−maleimide chemistry in aqueous conditions at neutral pH. The site selectivity of this reaction was confirmed using trypsin digest, as reported previously.[20] The protein concentration was determined using a Bradford assay,[27] which allowed mixing of monomer batches in the desired ratios. Monomers were then assembled into rods by equilibration in 100 mM phosphate buffered at pH 5.5. Changes in assembly state were monitored using size exclusion chromatography (data not shown).

A comparison of the steady-state fluorescence emission spectra (Figure 2a) of assemblies **1** and **2** indicates that energy transfer occurs from OG to AF. Upon excitation of **2** at donor wavelengths (460 nm), a distinct emission band at 617 nm is observed that is absent from the emission spectrum of **1**, suggesting that the new peak originates from AF emission due to Förster resonance energy transfer (FRET). Consistent with previous reports, the presence of a large donor emission band in **2** suggests that energy transfer from OG to AF is incomplete in the 100:1 system.[20] This is due to the fact that the spectral overlap between OG and AF is relatively small. Previously, systems with increased spectral overlap due to the inclusion of a third chromophore that absorbs in the intermediate region (tetramethylrhodamine, $\lambda_{Abs} = 517$ nm) were shown to exhibit efficiencies over 90%. However, the high degree of overlap between the emission bands in this three-chromophore system was found to complicate the analysis of time-resolved fluorescence data; hence, the more spectrally resolved (but less efficient system) is described here.

Initial experiments that directly probed the temporal evolution of donor emission of assemblies **1** and **2** at 524 nm seemed to suggest the occurrence of energy transfer in **2**. As shown in Figure 2b, the distinction between the two kinetic profiles is striking: the decay of OG emission in rods containing acceptor (**2**) is much more rapid than in rods containing only the donor (**1**). The simplest explanation for this observation is the presence of an additional decay channel in **2**; that is, energy transfer from OG to AF. Quantitative analysis of the kinetics was performed by deconvolution data fitting, which employs multiexponentials as a model function and explicitly takes the finite temporal response into account. We found that the data obtained for **1** can be satisfactorily described by a biexponential decay function with decay times (and relative amplitudes) of 995 ps (0.27) and 4.14 ns (0.73), respectively. To fit the data obtained for **2**, a model function consisting of three exponential terms is required. The rapid decay in this case is best characterized by two dominant components with decay times (and relative amplitudes) of 102 (0.65) and 323 ps (0.25), respectively. A minor, slow decay component of 4.59 ns is also needed, which accounts for a 10% relative amplitude. Because of this complicated, multiexponential decay behavior, it is not possible to assign any of these determined decay times to the donor-to-acceptor energy transfer.

The energy transfer from OG to AF in **2** should give rise to an increase in the AF emission with time. Thus, probing the temporal evolution of the AF emission is expected to allow a direct quantification of the time scale characteristic for the transfer process. Measurements in the acceptor emission band were performed at 600, 617, 650, and 685 nm. However, none of these kinetic profiles exhibited an observable rise. As an example, the data collected at 617 nm are shown in the inset of Figure 2b. These data can be best described by a sum of three exponential decay components with time scales (and relative amplitudes) of 418 ps (0.30), 1.95 ns (0.31), and 4.27 ns (0.39), respectively. The absence of a kinetic rise in the acceptor emission band seems to suggest either a lack of energy transfer from OG to AF or that the transfer time is too short to be resolved. The latter conclusion is clearly inconsistent with the measurement of the rapid donor decay kinetics (Figure 2b, solid line), the shortest decay times of which are clearly longer than our instrumental response function.

The seemingly contradictory results obtained from the kinetics of donor and acceptor emission arise from the very broad donor emission spectrum, which extends to the spectral region of the acceptor emission (Figure 2a). This leads to complex kinetics that result from contributions by both OG and AF at any detection wavelength within the AF emission band. As a result, the decrease in the donor fluorescence makes the concomitant increase in the acceptor emission to be indistinguishable. To prove qualitatively that energy transfer indeed occurs from donor to acceptor in **2**, time-resolved emission spectra were reconstructed from 10 kinetic profiles measured at different wave-

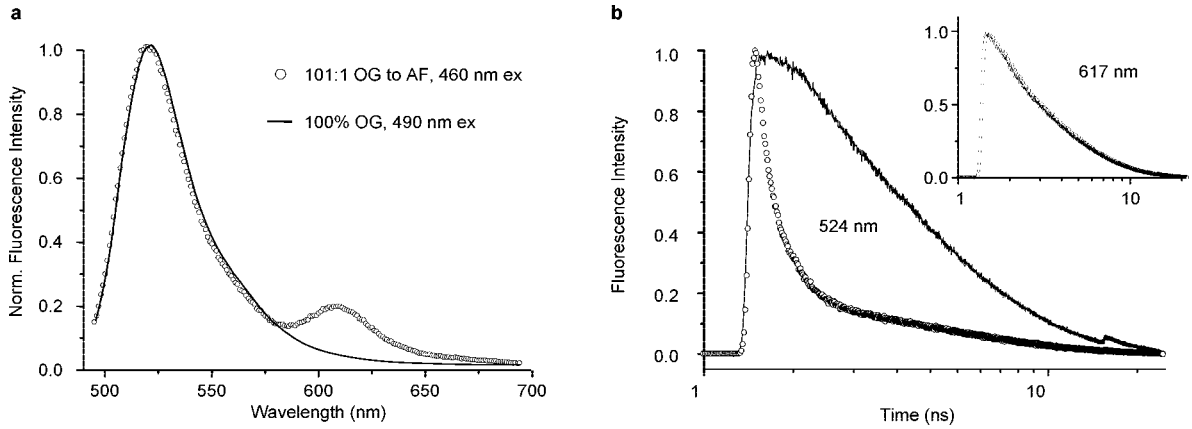

Figure 2. Steady-state and time-resolved emission of rods with and without acceptor chromophores. (a) Steady-state fluorescence emission spectra of the 100% donor OG rods (solid black line) and rods consisting of a 100:1 ratio of OG to AF (open circles). The two spectra are scaled to equal amplitude at 524 nm. (b) Normalized fluorescence kinetics at 524 nm for rods containing donor only (solid black line) or a 100:1 ratio of OG to AF (open circles). The inset shows kinetic data of the mixed chromophore system measured at the acceptor emission band (617 nm).

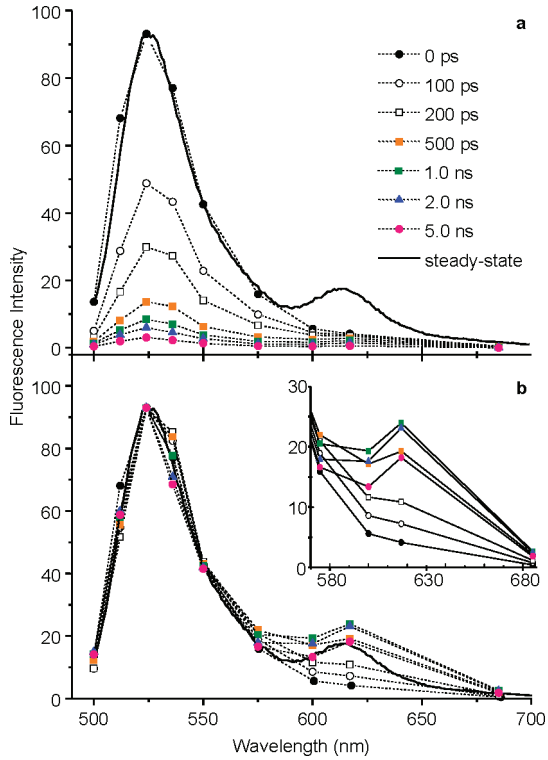

Figure 3. (a) Reconstructed time-resolved fluorescence emission spectra at times ranging from 0 ps to 5.0 ns. The solid black line shows the steady-state emission spectrum. (b) The identical spectra from part **a** normalized at 524 nm to observe changes in the intensity of AF emission. Inset: an expanded view of the spectral evolution in acceptor band.

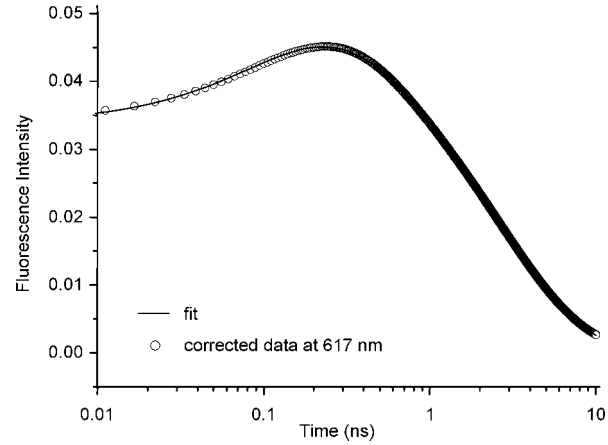

Figure 4. Calculated kinetic difference profile using the experimental data collected at 617 and 575 nm (open circles). The solid line is the fit (see text).

lengths ranging from 500 to 685 nm. This reconstruction involved calculating the decay profiles according to the deconvolution fitting results (decay times, relative amplitudes, and constant small background) and scaling their time integrals according to the corresponding intensities of the steady-state emission spectrum (Figure 2a, open circles). Figure 3a shows an overlay of the spectra obtained by this approach, together with the steady-state fluorescence emission spectrum. Consistent with the representative kinetics shown in Figure 2b, the amplitudes of these reconstructed spectra decrease with time in spectral regions of both the donor and acceptor emission.

The temporal evolution of acceptor emission can be qualitatively visualized by artificially "keeping" the donor emission constant. This is realized by normalizing the spectra shown in Figure 3a at 524 nm. As shown in Figure 3b, a clear increase in the donor emission intensity with time is evident within ~1 ns, after which the emission begins to decrease. While this treatment allows for the visualization of energy transfer, it precludes extracting the rate of transfer from the change in acceptor intensity. This is because normalizing at the donor emission wavelength is equivalent to dividing the acceptor kinetics by the donor decay at a given detection wavelength. It leads to a significantly slower kinetic rise of the acceptor fluorescence than the one that arises from the actual transfer event.

Instead, a refined estimate of the time scale of energy transfer between OG and AF can be obtained by carefully subtracting the donor contribution from the kinetics measured at 617 nm. In view of the wavelength dependence of OG kinetics, which will be discussed in more detail later, data measured at 575 nm were used to approximate the donor decay at 617 nm. This wavelength was selected because it is close to the emission band of the acceptor but has negligible contribution from it. Prior to subtraction, the two kinetic profiles were first scaled such that their time integrals were proportional to the steady-state emission intensities of **1** and **2** at 617 nm. The resulting difference profile is shown in Figure 4. In contrast to the data measured at 617 nm (Figure 2, inset), the difference exhibits a clear rise with a time scale of 113 ps.

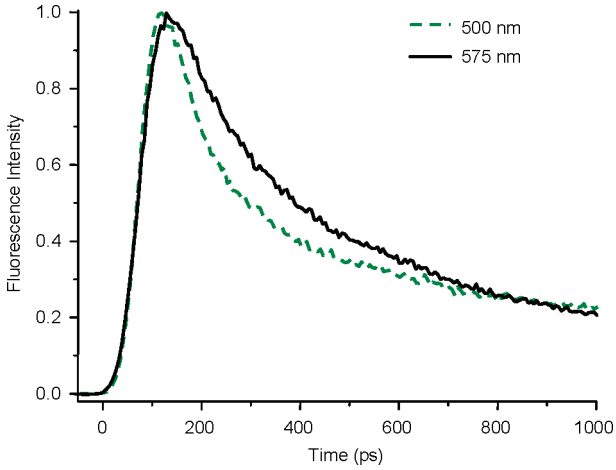

Figure 5. Normalized fluorescence kinetics detected for **2** at 500 (dashed green line) and 575 nm (black line). Only the initial parts of the data are shown to highlight the dependence of the fastest decay constant on detection wavelength.

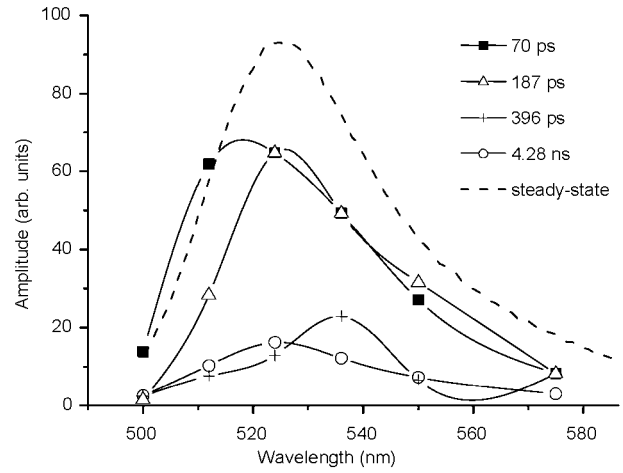

Figure 6. DAS calculated in the OG emission band for the 100:1 OG to AF rod system. The dashed line indicates the corresponding steady-state fluorescence emission spectrum.

This time scale should be considered as a lower limit of the actual transfer time due to the following reasons. First, analysis of the data measured on a sample of 100% AF-labeled monomers at 617 nm shows that a fast decay of 146 ps with a small relative amplitude of 5% is needed to describe the fluorescence decay of the AF chromophore properly. The presence of such a fast decay component would shorten the time scale of the rise component of assembly **2**. Second, the donor decay at 617 nm may be slower than the one at 575 nm, also contributing to a slower rise than the one calculated based on the difference profile shown in Figure 4.

Although the analysis described above yields a clear picture of energy transfer in terms of the AF acceptor, identification of the transfer time from the corresponding donor decays is complicated by the fact that the kinetics of the OG emission band depend on the detection wavelength. This wavelength dependence is manifested by significantly increased time scales of the dominant decay components with increasing wavelength. For instance, the fastest decay component of OG emission is found to increase from 56 ps at 500 nm to 139 ps at 575 nm (Figure 5). This dependence indicates that the contribution of donor-to-donor energy transfer to the kinetics varies at different wavelengths. The donor molecules absorbing at shorter wavelengths have a higher probability of transferring excitation energy to those absorbing at longer wavelengths. Similar intraband transfer processes have been observed in natural photosynthetic LH complexes composed of weakly interacting BChls, such as in the B800 molecules of the peripheral LH complex of purple bacteria.[5,10] Additionally, both short- and long-wavelength-absorbing donor molecules can transfer energy to the acceptor, provided they are nearby.

Concurrent donor-to-donor transfer prohibits the extraction of both the time scale and the efficiency for the donor-to-acceptor transfer through the analysis of individual kinetic profiles detected in the OG emission band. A global lifetime analysis[24] was therefore performed for the data collected at 500, 512, 524, 536, 550, and 575 nm. In this analysis, the lifetimes of corresponding decay components were linked together, but the amplitudes were treated as local parameters. To describe the behavior of assembly **2** accurately, we found that a model function consisting of four exponential components was needed. The corrected wavelength dependence of the resulting amplitudes was plotted as decay-associated spectra[25] (DAS) in Figure 6. The quality of the fits was judged by the obtained weighted residuals (global and local chi-square (χ^2) values). As shown in Figure 6, the two DAS with lifetimes of 70 and 187 ps have dominant amplitudes. Although both DAS may be assigned to the energy transfer from donor to acceptor, good agreement with the rise shown in Figure 4 makes the DAS with a lifetime of 187 ps a more favorable choice. Following this assignment, we further estimated the transfer efficiency from the ratio of the area under the DAS with 187 ps lifetime to the sum of areas under all four DAS, resulting in a value of 36%. This result is nearly identical to the 34% efficiency determined from the measurement of the steady-state fluorescence−excitation spectrum, strongly supporting our assignment of the 187 ps component to donor-to-acceptor energy transfer.

On closer inspection of the DAS shown in Figure 6, we find that the one associated with the 70 ps component is more pronounced at shorter wavelengths, suggesting that this decay component arises from energy transfer between donor molecules. The longest decay time (4.28 ns) is very similar to the lifetime (4.04 ns) determined for an aqueous solution of OG chromophores at neutral pH.[28] This similarity indicates that this decay component originates from a small number of donor molecules that are disconnected in terms of energy transfer from a functional network. At this point, the origin of the 396 ps component is unclear, although one possibility is that it indicates energy transfer between nonadjacent donor and acceptor molecules.

In conclusion, we have studied excitation energy transfer processes in TMV assemblies using picosecond time-resolved fluorescence. We found the energy transfer from OG to AF occurs in 187 ps with an efficiency of 36%. A faster decay component of 70 ps was also observed from global lifetime analysis and is attributed to donor-to-donor transfer. Although these values are significantly slower than those found in natural systems, they compare well to other artificial systems, and they provide a useful benchmark for synthetic arrays based on self-assembling protein scaffolds.[21–23,29,30] Through improvements in spectral matching between the donor and acceptor chromophores, increases in these rates are anticipated. Because synthetic systems based on other organic chromophores are also likely to exhibit broad and potentially overlapping spectral properties, the analysis techniques reported here are likely to be of use to many groups seeking to evaluate them.

Experimental

Construction of TMVP Expression Plasmids. pTMV0041, a wild-type TMV cDNA clone, was received as a gift from Dr. Dennis Lewandowski, University of Florida. Standard recombinant techniques were used to construct an expression plasmid with pET20b vector DNA (Novagen). The TMVP gene was amplified by PCR, using an upstream primer with the sequence 5′-GATTCGTTTTACATATGTCTTAC-3′ and a downstream primer with the sequence 5′-TAGTACCATGGCATCTTGACTAC-3′. The amplification product was digested with NdeI and NcoI (NEB) before ligation into pET20b with T4 DNA ligase (NEB). A TMVP-S123C mutant construct was made using standard recombinant techniques.

Expression and Purification of Recombinant TMV Coat Protein (TMVP). TMVP was expressed and purified according to a modified literature procedure.[31] Tuner DE3pLysS competent cells (Novagen) were transformed with pTMVP, and colonies were selected for inoculation of Terrific Broth cultures. When cultures reached midlog phase as determined by OD 600, expression was induced by addition of 10 μM IPTG (Invitrogen). Cultures were grown 14−18 h at 30 °C, harvested by centrifugation, and stored at −80 °C.

Induced cells were thawed and resuspended in ice-cold buffer A (20 mM Tris, pH = 7.2; 5 mM DTT; 20 mM NaCl) containing 1 mM Pefabloc SC (Roche). Cells were lysed by sonication (Branson Ultrasonics), and the resulting lysate was cleared by ultracentriguation for 50 min at 40 000 rpm in a Beckman 40 Ti rotor. The cleared lysate was applied to a DEAE anion-exchange column (Amersham) and eluted with buffer A at 4 °C. Fractions were analyzed by SDS−PAGE, and fractions containing TMVP were combined, concentrated, and dialyzed against 50 mM sodium citrate buffer, pH = 3.5. The resulting TMVP precipitate was collected by centrifugation, washed with additional citrate buffer, and resuspended in buffer B (100 mM Tris, pH 8). The purified TMVP was quantified by Bradford assay,[26] flash-frozen, and stored at −20 °C.

General Procedure for Chromophore Attachment. A thawed aliquot of TMVP (8.0 mg/mL in 100 mM HEPES buffer, pH 6.5, 1% TCEP) was exchanged into 100 mM KH_2PO_4, pH 7, using a NAP-10 column. The solution was diluted to 1.5 mg/mL in TMVP, and 5 equiv of maleimide-functionalized chromophore were added as a DMF solution (up to 5%, v/v). In optimization experiments, the higher DMF concentrations, increased equivalents of the dye, or extended reaction times led to overlabeling, presumably at the native C27 residue. The reaction mixture was vortexed briefly and left at room temperature for 15−20 min. The reaction was quenched with 20 equiv of β-mercaptoethanol, and the mixture was passed through a NAP-10 column to remove excess chromophore. Conversion of TMVP to modified product was monitored by LC/ESI-MS and UV−visible spectroscopy. Reactions involving smaller molecular weight dyes, such as Oregon Green 488, required a shorter reaction time as compared to those involving larger dyes, such as Alexa Fluor 594. The site selectivity of the modification reaction was confirmed through mass spectrometry analysis of peptide fragments after digestion with trypsin.[20]

Assembly of TMVP Disks and Rods. Solutions of dye-modified TMVP monomers were diluted to 0.75 mg/mL and dialyzed overnight against 25 mM phosphate buffer, pH 8, to achieve equilibration to the monomer state.[16] After dialysis, TMVP mixtures were analyzed by size exclusion chromatography using an HPLC equipped using a Phenomenex PolySep-GFC-P 5000 column (300 × 7.8 mm, flow rate 1.0 mL/min) equilibrated with 25 mM phosphate buffer, pH 8. The concentration of dye-modified TMVP monomers was quantified using a Bradford assay.[19]

The monomers were combined in the stoichiometric ratios and allowed to equilibrate for 3 h at room temperature to allow for exchange between any preformed small aggregates before assembly. For assembly into rods, monomer solutions were exchanged into 100 mM sodium acetate buffer, pH 5.5, and dialyzed overnight. After dialysis, the conversion to larger structures was monitored by size exclusion chromatography, and the assemblies were characterized visually using TEM.

Ultrafast Spectroscopy. Time-resolved fluorescence measurements were performed using a single-photon counting apparatus set at the magic angle polarization.[32] A commercial mode-locked femtosecond laser (Mira 900F, Coherent) pumped by a diode-pumped, frequency-doubled Nd:YVO_4 laser (Verdi V-10, Coherent) was used as an excitation source. The output of the laser was frequency-doubled using a 1.5-mm-thick BBO crystal. The repetition rate was reduced to 3.76 MHz using an extra-cavity pulse picker. Excitation was at 465 nm with a pulse energy of ∼0.1 nJ. Fluorescence emission was selected using a single grating monochromator (H20 VIS, Horiba Jobin Yvon) with a bandwidth of 4 nm and detected with a microchannel plate photomultiplier (Hamamatsu R3809U-51). The instrumental response function was ∼70 ps (full width at the half-maximum), and a channel resolution of 5.56 ps was chosen for all the measurements reported in this paper. Typically, more than 10 000 counts were collected in the peak channel to obtain a good signal-to-noise ratio.

Acknowledgment. Y.Z.M. and G.R.F. wish to thank the NSF for support. We gratefully acknowledge the Biomolecular Materials Program at Lawrence Berkeley National Labs and the Berkeley Chemical Biology Graduate Program (NRSA Training Grant 1 T32 GMO66698) for generous financial support. R.A.M. acknowledges the NSF IGERT program (DGE-0333455) for a graduate fellowship. The global lifetime analysis was performed using the Globals software package developed at the Laboratory for Fluorescence Dynamics at the University of Illinois at Urbana−Champaign.

References and Notes

(1) Nelson, N.; Ben-Shem, A. *Nat. Rev. Mol. Cell Biol.* **2004**, *5*, 971–982.
(2) van Grondelle, R.; Dekker, J. P.; Gillbro, T.; Sundstrom, V. *Biochim. Biophys. Acta* **1994**, *1187*, 1–65.
(3) Sundstrom, V.; Pullerits, T.; van Grondelle, R. *J. Phys. Chem. B* **1999**, *103*, 2327–2346.
(4) Fleming, G. R.; van Grondelle, R. *Curr. Opin. Struct. Biol.* **1997**, *7*, 738–748.
(5) van Grondelle, R.; Novoderezhkin, V. I. *Phys. Chem. Chem. Phys.* **2006**, *8*, 793–807.
(6) McDermott, G.; Prince, S. M.; Freer, A. A.; Hawthornthwaitelawless, A. M.; Papiz, M. Z.; Cogdell, R. J.; Isaacs, N. W. *Nature* **1995**, *374*, 517–521.
(7) Koepke, J.; Hu, X. C.; Muenke, C.; Schulten, K.; Michel, H. *Structure* **1996**, *4*, 581–597.
(8) Roszak, A. W.; Howard, T. D.; Southall, J.; Gardiner, A. T.; Law, C. J.; Isaacs, N. W.; Cogdell, R. J. *Science* **2003**, *302*, 1969–1972.
(9) Scheuring, S.; Seguin, J.; Marco, S.; Levy, D.; Robert, B.; Rigaud, J. L. *Proc. Natl. Acad. Sci. U.S.A.* **2003**, *100*, 1690–1693.
(10) Ma, Y.-Z.; Cogdell, R. J.; Gillbro, T. *J. Phys. Chem. B* **1998**, *102*, 881–887.
(11) Agarwal, R.; Rizvi, A. H.; Prall, B. S.; Olsen, J. D.; Hunter, C. N.; Fleming, G. R. *J. Phys. Chem. A* **2002**, *106*, 7573–7578.
(12) Pullerits, T.; Sundstrom, V. *Acc. Chem. Res.* **1996**, *29*, 381–389.
(13) Wasielewski, M. R. *J. Org. Chem.* **2006**, *71*, 5051–5066.
(14) Noy, D.; Moser, C. C.; Dutton, P. L. *Biochim. Biophys. Acta* **2006**, *1757*, 90–105.
(15) Balaban, T. S. *Acc. Chem. Res.* **2005**, *38*, 612–623.
(16) Alstrum-Acevedo, J. H.; Brennaman, M. K.; Meyer, T. J. *Inorg. Chem.* **2005**, *44*, 6802–6827.

(17) Gust, D.; Moore, T. A.; Moore, A. L. *Acc. Chem. Res.* **2001**, *34*, 40–48.

(18) Cogdell R. J. LindsayJ. G. *Trends Biotechnol. 16*521527.

(19) Hammarstrom, L. *Curr. Opin. Chem. Biol.* **2003**, *7*, 666–673.

(20) For additional examples of materials constructed using the TMV coat protein, see:(a) Shenton, W.; Douglas, T.; Young, M.; Stubbs, G.; Mann, S. *Adv. Mater.* **1999**, *11*, 253. (b) Knez, M.; Sumser, M.; Bittner, A. M.; Wege, C.; Jeske, H.; Martin, T. P.; Kern, K. *Adv. Funct. Mater.* **2004**, *14*, 116–124. (c) Schlick, T. L.; Ding, Z. B.; Kovacs, E. W.; Francis, M. B. *J. Am. Chem. Soc.* **2005**, *127*, 3718–3723. (d) Holder, P. G.; Francis, M. B. *Angew. Chem., Int. Ed.* **2007**, *46*, 4370–4373. (e) Niu, Z.; Liu, J.; Lee, L. A.; Bruckman, M. A.; Zhao, D.; Koley, G.; Wang, Q. *Nano Lett.* **2007**, *7*, 3729–3733. (f) Yi, H. M.; Nisar, S.; Lee, S. Y.; Powers, M. A.; Bentley, W. E.; Payne, G. F.; Ghodssi, R.; Rubloff, G. W.; Harris, M. T.; Culver, J. N. *Nano Lett* **2005**, *5*, 1931–1936. (g) Vega, R. A.; Maspoch, D.; Salaita, K.; Mirkin, C. A. *Angew. Chem., Int. Ed.* **2005**, *44*, 6013–6015. For materials constructed using other viruses, see: (h) Douglas, T.; Young, M. *Nature* **1998**, *393*, 152–155. (i) Wang, Q.; Lin, T. W.; Tang, L.; Johnson, J. E.; Finn, M. G. *Angew. Chem., Int. Ed.* **2002**, *41*, 459–462. (j) Mao, C. B.; Solis, D. J.; Reiss, B. D.; Kottmann, S. T.; Sweeney, R. Y.; Hayhurst, A.; Georgiou, G.; Iverson, B.; Belcher, A. M. *Science* **2004**, *303*, 213–217. (k) Medintz, I. L.; Sapsford, K. E.; Konnert, J. H.; Chatterji, A.; Lin, T. W.; Johnson, J. E.; Mattoussi, H. *Langmuir* **2005**, *21*, 5501–5510. (l) Soto, C. M.; Blum, A. S.; Vora, G. J.; Lebedev, N.; Meador, C. E.; Won, A. P.; Chatterji, A.; Johnson, J. E.; Ratna, B. R. *J. Am. Chem. Soc.* **2006**, *128*, 5184–5189. (m) Scolaro, L. M.; Castriciano, M. A.; Romeo, A.; Micali, N.; Angelini, N.; LoPasso, C.; Felici, F. *J. Am. Chem. Soc.* **2006**, *128*, 7446–7447.

(21) Miller, R. A.; Presley, A. D.; Francis, M. B. *J. Am. Chem. Soc.* **2007**, *129*, 3104–3109.

(22) Endo, M.; Fujitsuka, M.; Majima, T. *Chem.−Eur. J.* **2007**, *13*, 8660–8666.

(23) Neuwahl, F. V. R.; Righini, R.; Adronov, A.; Malenfant, P. R. L.; Frechet, J. M. J. *J. Phys. Chem. B* **2001**, *105*, 1307–1312.

(24) Adronov, A.; Gilat, S. L.; Frechet, J. M. J.; Ohta, K.; Neuwahl, F. V. R.; Fleming, G. R. *J. Am. Chem. Soc.* **2000**, *122*, 1175–1185.

(25) Beechem, J. M.; Gratton, E. Time-Resolved Laser Spectroscopy in Biochemistry. *Proc. SPIE, Int. Soc. Opt. Eng.* **1988**, 909.

(26) Holzwarth, A. R. In *Biophysical Techniques in Photosynthesis*; Amesz, J., Hoff, A. J., Eds.; Kluwer Academic Publishers: Dordrecht, 1996.

(27) Bradford, M. *Anal. Biochem.* **1976**, 248.

(28) Orte, A.; Crovetto, L.; Talavera, E. M.; Boens, N.; Alvarez-Pez, J. M. *J. Phys. Chem.* **2005**, *109*, 734–747.

(29) Kleiman, V. D.; Melinger, J. S.; McMorrow, D. *J. Phys. Chem. B* **2001**, *105*, 5595–5598.

(30) Sessler, J. L.; Wang, B.; Harriman, A. *J. Am. Chem. Soc.* **1995**, *117*, 704–714.

(31) Shire, S. J.; McKay, P.; Leung, D. W.; Chachianes, G. J.; Jackson, E.; Wood, W. I. *Biochemistry* **1990**, *29*, 5119–5126.

(32) Yang, D. D. H.; Yang, N. C. C.; Steele, I. M.; Li, H.; Ma, Y. Z.; Fleming, G. R. *J. Am. Chem. Soc.* **2003**, *125*, 5107–5110.

JP8006393